Research article

Co^{2+} and Cr^{3+} ions removal from wastewater by using nanostructural hydroxyapatite

Nguyen Thu Phuong[1*], Nguyen Thi Thom[1], Pham Thi Nam[1], Nguyen Van Trang[1],
Tran Thi Thu Huong[2], Do Thi Hai[2], Le Phuong Thu[3], Magdalena Osial[4,5], Dinh Thi Mai Thanh[1,3*]

[1]Institute for Tropical Technology, Vietnam Academy of Science and Technology, 18 Hoang Quoc Viet, Cau Giay, Hanoi 10072, Viet Nam

[2]Hanoi University of Mining and Geology, 18 Pho Vien, Duc Thang, Bac Tu Liem, Hanoi 10000, Viet Nam

[3]University of Science and Technology of Hanoi, Vietnam Academy of Science and Technology, 18 Hoang Quoc Viet, Cau Giay, Hanoi 10072, Viet Nam

[4]Faculty of Chemistry, University of Warsaw, Pasteura 1, Warsaw 02-093, Poland

[5]Department of Theory of Continuous Media and Nanostructures, Institute of the Fundamental Technological Research, Polish Academy of Sciences, Pawińskiego 5B Str., Warsaw 02-106, Poland

Abstract

Due to the growing pollution of the environment, water purification methods have to be improved. One of the most effective solutions is the removal of heavy metal ions by porous materials, including hydroxyapatite. Lao Cai Province in Vietnam has a tremendous reservoir of apatite ore that can be a precursor for nanostructural materials. In this paper, we refer to the recent studies on removing heavy metal salts, including the cobalt and chromium ions, from the wastewater by the nanostructural hydroxyapatite obtained from the apatite ore gained in the Lao Cai Province. The measurements were performed according to the pH, mass of the adsorbent addition into the real wastewater solution, and time exposition onto the adsorbent; and the suitable condition is a dose of modified apatite of 1 g/L; contacting time of 60 minutes and 6 g/L and 15 minutes in the pH range from pH$_0$ (3.76 and 6.57) to neutral pH corresponding to Cr^{3+} and Co^{2+}. We show that just a small amount of the nanostructural hydroxyapatite can work efficiently to remove the chromium and cobalt ions from the solution with maximum adsorption capacity is 70.37 mg/g and 13.52 mg/g, respectively.

Keywords. Nanostructural hydroxyapatite, apatite ore, wastewater treatment, heavy metal ions removal, novel ecofriendly adsorbent.

1. INTRODUCTION

Water is an essential molecule for living on Earth. Recently, due to the growing industrialization, its reservoirs are widely polluted with many chemical compounds, including heavy metals. One of them that has adverse effects on health is cobalt and chromium. Its appearance in the environment is mainly caused by anthropogenic activities like in the battery and electronic industries.[1] The presence of chromium and cobalt in the environment can be fatal for living organisms leading to adverse health effects.[2-5] Their presence in drinking water is one of the oldest and most challenging pollution problems that affect human health and ecosystems. These metals cause serious problems including cancerogenic effects on the body. For example,

contact in a short time with high content of chromium can lead to irritation at the point of contacts such as nasal mucosa and skin. Exposure to Cr(III) at a high level causes skin rash and it can accumulate in the human cells leading to DNA destruction, affecting the respiratory tract, increase in lung weight, and having an immunological effect as a toxic. Exposure to a high amount of cobalt cause problem with fetus development during the third month. Cobalt was supposed that it may be a carcinogen by many researchers.

For that reason, it is crucial to deal with the removal of heavy metals from aquatic reservoirs. Besides many techniques, the coagulation, electro-coagulation, electrodialysis, flocculation, ion exchange, chemical precipitation, membrane separation, reverse osmosis, photocatalytic removal

Wiley Online Library © 2022 Vietnam Academy of Science and Technology, Hanoi & Wiley-VCH GmbH

of heavy metal, solvent extraction for heavy metal removal, and the adsorption of the heavy metals by the adsorbents seems to be a promising and effective technique of adsorption.[6-9] Adsorption method has easy operational conditions, low-cost, has a wide pH range, and has extraordinary metal binding capacities. The adsorption method based on natural sorbents is used widely for its simplicity, low costs, and high efficiency.[10-12] Among many materials that are used for sorption like activated carbon,[13-15] carbon nanotubes,[13] clays,[13,16] zeolites,[13,14] bio-adsorbents,[10,13] silica,[15,17] wood ash,[4] and apatite,[10-12,18-24] the hydroxyapatite have promising properties for the heavy metals removal from the wastewater. The hydroxyapatite (HAp) having the formula $(Ca_{10}(PO_4)_6(OH)_2)$ can occur in different forms like the bare HAp, fluorapatite $(Ca_{10}(PO_4)_6F_2)$, and chlorapatite $(Ca_{10}(PO_4)_6Cl_2)$. Each form can be easily used for aquatic pollution removal. This mineral offers a large surface for removing many chemical compounds from aqueous media and biocompatibility, being non-toxic for living organisms. Due to its physico-chemical properties it is widely synthesized to be used for adsorption of many inorganic compounds like heavy metal ions such as Cu^{2+},[11,19] Zn^{2+},[19] Cd^{2+},[10,11] Co^{2+}, Ni^{2+}, Hg^{2+},[22,25] Cr^{6+},[21] Ag^+,[18] Pb^{2+},[12,14] Fe^{3+} and Cr^{3+}.[3,22] Hydroxyapatite also has tremendous potential for the removal of anions like As^{3-},[24] F^-,[26,27] organic pollutants like phenol,[18,23] nitrobenzene,[28] and even antibiotics with high adsorption ability.[29-31] Hydroxyapatite can be synthesized from chemical sources or obtained from natural sources such as animal bones;[12,25] however, it can also be easily prepared from the natural apatite ores.[11] An enormous abundance of apatite ore, even 2.55 billion tons of the apatite, making it a low-cost and promising source of hydroxyapatite for wastewater treatment, especially the water reservoirs polluted with cobalt and chromium ions was found in Lao Cai province, Vietnam. This approach is still relatively new with only a few studies done before.[11,32]

In this work, the nanostructural hydroxyapatite was obtained within the chemical modification of natural apatite ore gained in the Lao Cai province as a low cost, natural, and eco-friendly adsorbent material for heavy metals treatment. We present the effective removal of the Co^{2+} and Cr^{3+} ions from the wastewater by the application of the hydroxyapatite, obtained from the natural apatite ore. The studies were performed in function of the pH of the tested solution, ions concentration, adsorbent mass, time, and temperature on adsorption capacity and efficiency.

2. MATERIALS AND METHODS

2.1. Materials, chemicals

The natural apatite ore was supplied from the Lao Cai province in Vietnam. The nitric acid, HNO_3, 63 %, ammonia solution $NH_{3(aq)}$ 25 %, cobalt(II) nitrate hexahydrate, $Co(NO_3)_2 \cdot 6H_2O$, 99 %, chromium(III) chloride, $CrCl_3$, 99 %, sodium hydroxide NaOH 96 %, and hydrochloric acid HCl 36 % were all analytical grade and purchased from Xilong Scientific Co, China.

2.2. Methods and equipment

The morphology of the modified ore was investigated with two techniques: the Scanning Electron Microscopy (SEM), JSM-6510LV, JEOL Ltd. (Japan) and Transmission Electron Microscopy (TEM) JEM-2100 JEOL Ltd. (Japan).

Modification of the apatite ore procedure: The apatite ore was modified following the procedure in the published article, the obtained material had a phase structure with a specific surface area of 100.79 $m^2 \cdot g^{-1}$ and pH_{pzc} of about 7.49.[11]

Modified apatite ore was characterized by the zeta potential by the Dynamic Light Scattering method (DLS, SZ-100V2, Nanoparticle analyzer, Nanopartica, Horiba Scientific (Japan) in the charge range of -200 to 200 mV at 25 °C).

The crystallinity of the modified apatite ore before and after the adsorption was characterized by the phase component by X-ray Diffraction (XRD), D8 ADVANCE-Bruker, CuK$_\alpha$ radiation (λ = 1.54056 Å) with a step angle of 0.030°, the scanning rate of 0.04285° per second, and 2θ degree was measured in the range of 10-70°.

2.3. Cobalt (Co^{2+}) and chromium (III) (Cr^{3+}) ions adsorption experiments

The Co^{2+} and Cr^{3+} ion adsorption experiments were carried out in 50 mL of $Co(NO_3)_2$ or $CrCl_3$ solution at concentrations ranging from 5 mg·L^{-1} to 370 mg·L^{-1}. A mass of modified apatite ore (from 0.005 g to 0.4 g) was introduced into the solution. Initial pH values of the solution ranged from 1.68 to 7.96 and were obtained using 0.01 M NaOH and 0.01 M HCl. A pH meter was used to control the pH of the solution. By using a magnetic stirrer at a rate of 400 rpm, the mixtures were stirred for various time intervals (5-90 minutes). Each experiment was repeated three times and the standard deviation is smaller than 5 %.

Co^{2+} and Cr^{3+} adsorption efficiency H (%) and

capacity (Q (mg·g⁻¹)) were determined by these following Eqs. (1) and (2):

$$H = (C_0 - C_e) \cdot \frac{100}{C_0} \qquad (1)$$

$$Q = (C_0 - C_e) \cdot \frac{V}{m} \qquad (2)$$

where C_0 (mg·L⁻¹) is the initial Co^{2+} and Cr^{3+} concentration in the solution, C_e (mg·L⁻¹) is the equilibrium heavy metal ions concentration after the adsorption process, V (L) is the solution volume (V = 50 mL), and m (g) is the mass of modified apatite ore.

The Co^{2+} and Cr^{3+} concentrations were determined by the AAS method at a wavelength of λ = 240.7 nm and λ = 357.9 nm, respectively, on Atomic Absorption Spectrometry (AAS) iCE 3500 Thermo Scientific (Germany).

3. RESULTS AND DISCUSSION

3.1. Morphology and surface potential of modified apatite ore investigation

The morphology of the modified apatite ore was investigated using a Scanning Electron Microscope (SEM) and a Transmission Electron Microscope (TEM). The SEM image reveals the uniform distribution of nanosized and grain-like structures, with sizes of about 20 nm. As can be seen in Fig. 1a, hydroxyapatite aggregates form clusters. Complementary to the SEM analysis, the TEM studies reveal a more detailed morphology of the sample. As shown in Fig. 1b, the modified apatite ore has a regular structure, where the average diameter of particles is about 25 nm. Particles have similar shapes and sizes within the whole sample. The aggregation of particles was observed because of the fast evaporation of a solvent from the suspension while drying; however, particular grains are clearly seen confirming the nanostructural character of the obtained product of chemical modification.

The density of charges existing on the surface of modified apatite ore affects its stability. By using zeta potential, the surface charge of the modified apatite ore can be determined. The material's stability in suspension can be significantly influenced by Zeta potential through electrostatic repulsion between the particles. The value of negative zeta potential is about -34±0.5 mV due to the presence of hydroxyl groups. These groups will interact strongly with the heavy metals cations leading to the adsorption ability of material which will be shown in the next part.[33]
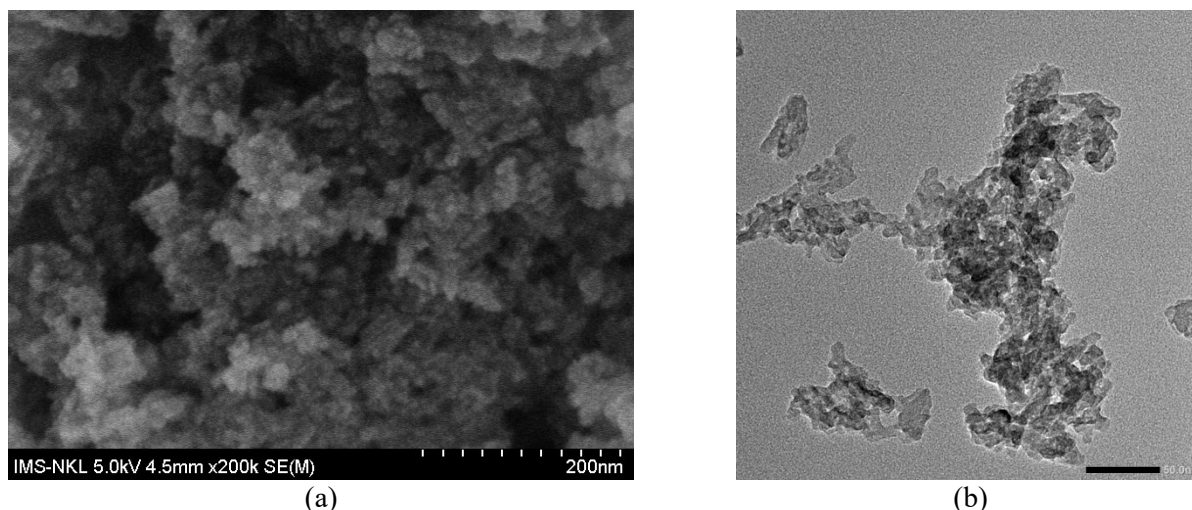

(a)   (b)

Figure 1: (a) SEM image and (b) TEM image of the modified apatite ore. The scale bar in the TEM image is about 50 nm

3.2. Calibration curve

Prior to the adsorption studies, the calibration curves were prepared. The solutions with initial Co^{2+} concentration from 0 to 10 mg·L⁻¹ and initial Cr^{3+} concentration from 0.4 to 8 mg·L⁻¹ were measured by AAS to obtain Abs values. The Abs values vary following Co^{2+} and Cr^{3+} concentrations were shown in Fig. 2. The calibration equation is a linear curve: $y = 0.02255x$, with correlation coefficient $R^2 = 0.99806$ and $y = 0.03974x$ ($R^2 = 0.99908$), which was used to determine the Co^{2+} and Cr^{3+} concentration in the subsequent experiments.

3.3. The effect of modified apatite ore mass

Figure 3 illustrates the effect of modified apatite ore mass on the capacity and efficiency of adsorption of

Co^{2+} and Cr^{3+}, with the mass of modified apatite ore ranging from 0.005 to 0.400 g and a contacting time of 60 minutes. Figure 3a shows that the adsorption efficiency rises rapidly from 60.00 % to 91.40 % when modified apatite ore mass increases from 0.100 g to 0.300 g, but from 0.300 g to 0.400 g the efficiency increases slowly, while the capacity decreases. The same behavior occurred with the Cr^{3+} adsorption process, see Fig. 3b. It can be explained as follow: When the mass of nano adsorbent increase, the particles will accumulate, and the distance between particles decreases leading to the screening effect. The binding sites for Cr^{3+}

molecules will be hidden by coacervates on the adsorbent surfaces. Furthermore, the overlap of the modified apatite ore leading to Cr^{3+} molecules will compete for available binding sites which have a limited number. At a larger dose of modified apatite ore, the aggregation or agglomeration also rises the Cr^{3+} diffusion path length, leading to the adsorption rate decrease. To conclude, 0.300 g and 0.050 g of modified apatite ore can be selected as suitable amounts for Co^{2+} and Cr^{3+} adsorption experiments to obtain not only a relatively high treatment efficiency but also a high adsorption capacity.
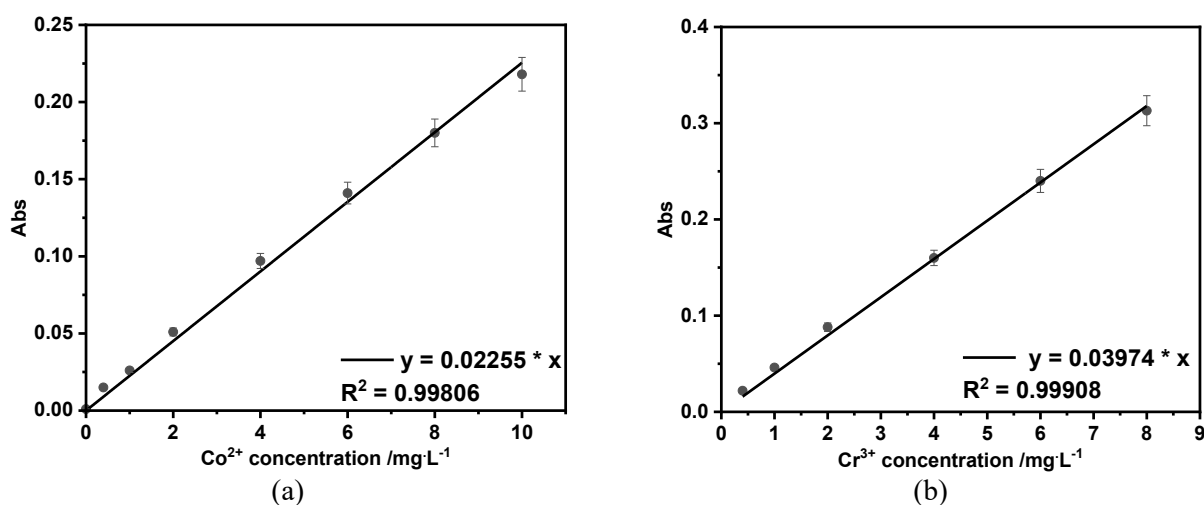

Figure 2: The calibration curves of (a) Co^{2+} and (b) Cr^{3+}

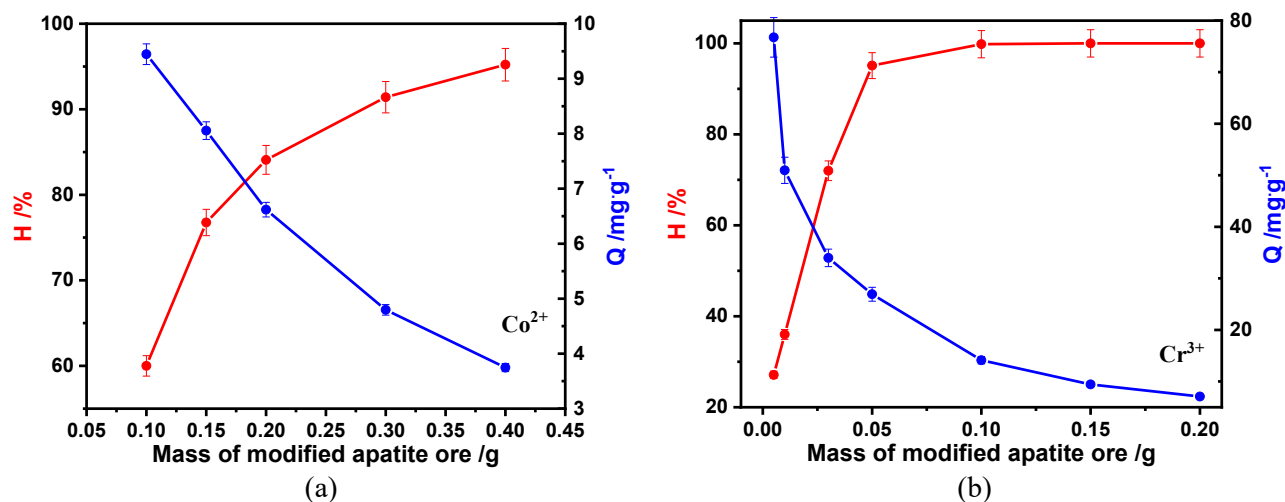*Figure 3:* The change of adsorption efficiency and capacity follows the mass of modified apatite ore
(at pH_0, $C_0 = 30$ mg·L⁻¹, contacting time is 60 minutes) for (a) Co^{2+} and (b) Cr^{3+}

3.4. The effect of contacting time

The next step was the investigation of the impact of different contacting times on the heavy metal ions' adsorption. Measurements were performed from 5 to 90 minutes, where results indicate an identical trend,

see Fig. 4 a,b. When the contacting time was increased from 5 to 15 minutes, the Co^{2+} adsorption efficiency increased from 71.30 % to 85.08 %, and the capacity rose from 4.66 mg·g⁻¹ to 5.57 mg·g⁻¹. In the range from 15 to 90 minutes, the adsorption efficiency and capacity increased slowly. This can

be explained as follows: when the contacting time increases, the heavy metal ions fill the pores and active sites of modified apatite ore more, leading to a rise in the adsorption efficiency and capacity. However, after a definite period, the adsorption equilibrium is gained and the adsorption capacity stays nearly unchanged. Therefore, 15 minutes is the

suitable contacting time for the Co^{2+} adsorption process. Similarly, for the removal of Cr^{3+} using modified apatite ore, 60 minutes was selected as the optimum, with the adsorption efficiency and capacity of Cr^{3+} of 89.16 % and 25.24 mg·g⁻¹, respectively.
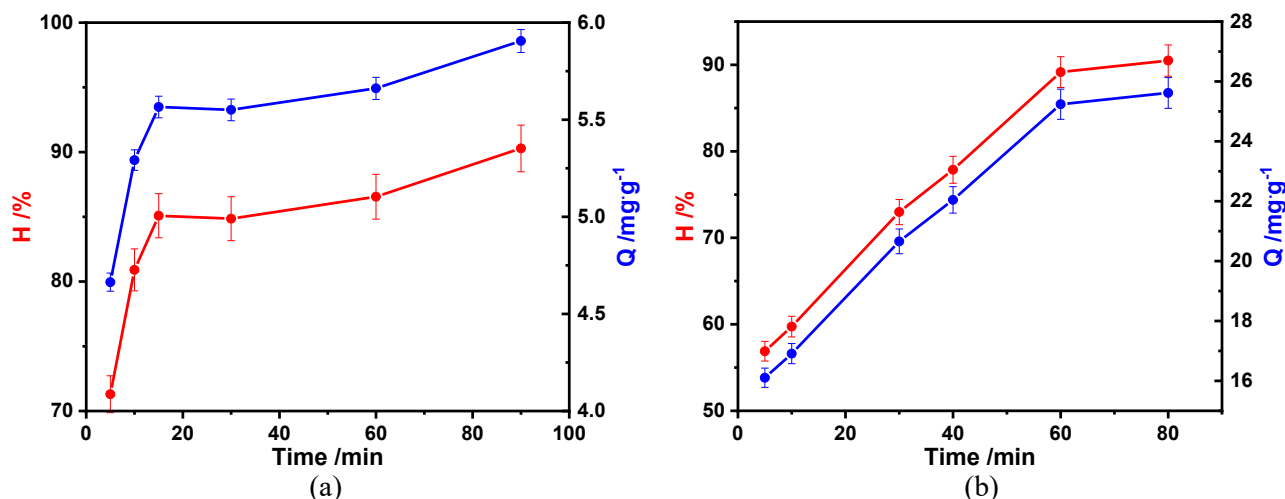

Figure 4: The variation of adsorption efficiency and capacity follow contacting time with $C_0 = 30$ mg·L⁻¹, pH_0, the mass of modified apatite ore is 0.3 g for (a) Co^{2+} and 0.05 g for (b) Cr^{3+}

3.5. The effect of pH

The pH of the initial solution in the adsorption process of modified apatite ore was varied from 3 to 8 for Co^{2+} and 1.68 to 5.6 for Cr^{3+}. The pH point zero charge (pHpzc) was determined to be 7.49.[7,11] Depending on the pH of the solution, the materials' surface has a negative or positive charge. If the adsorption process is conducted in pH solution < pHpzc 7.49, the surface of the material has a positive charge, and conversely, for pH solution > 7.49, the

surface of the adsorbent has a negative charge. From the pHpzc value, the adsorption ability of the material can be explained depending on the pH of the solution. However, when raising the pH of the Co^{2+} solution above 8, the precipitation appeared, and this also happened with Cr^{3+} at pH above 5.6. This explains why the experiment stopped at those pH points.

According to figure 5, the lower the pH level, the less effective the adsorption process is due to the competition between H^+ and heavy metal ions.

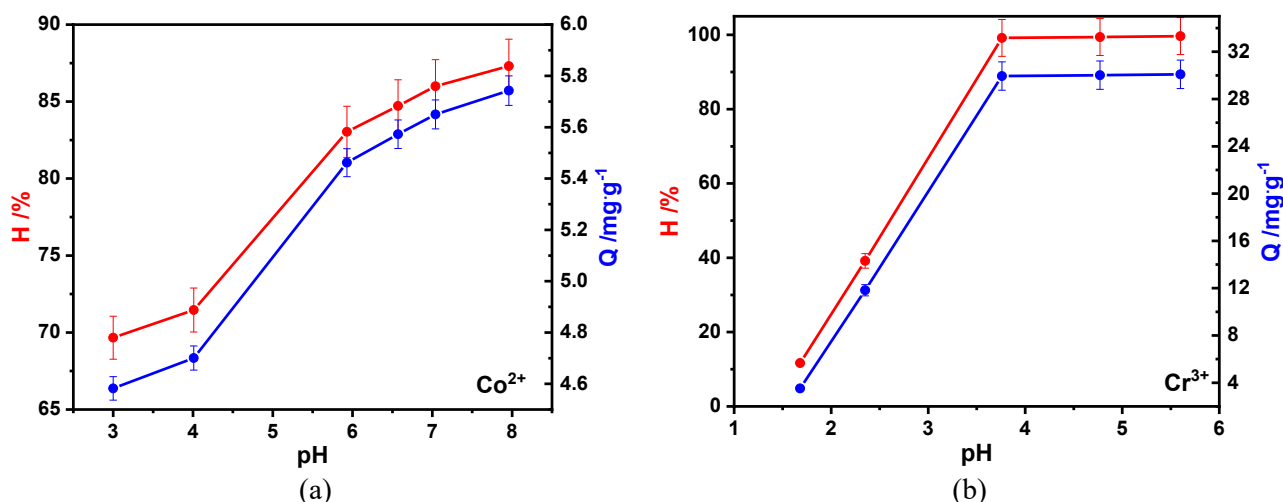*Figure 5:* The variation of adsorption efficiency and capacity follow pH with mass of modified apatite is about 0.3 g, $C_0 = 30$ mg·L⁻¹, contacting time is about 15 minutes for (a) Co^{2+} and mass of modified apatite is about 0.05 g, $C_0 = 30$ mg·L⁻¹, contacting time is about 60 minutes for (b) Cr^{3+}

When the pH solution increases, the efficiency and the adsorption capacity rise. When pH is lower than pHpzc, the surface of modified apatite ore has a positive charge, so the electrostatic force is the interactive force. When pH is higher than pHpzc, the efficiency and adsorption capacity increase, this can be explained as follow: at a high pH value, the surface of the material has a negative charge but if pH is too high then OH^- ions will lead to the formation of precipitation of $Co(OH)_2$ and $Cr(OH)_3$. In conclusion, pH = pH_0 of both Co^{2+} (6.57) and Cr^{3+} (3.76) were chosen to use in future experiments for practical applications.

3.6. Initial Co^{2+} and Cr^{3+} concentration effect

The following step was the determination of the influence of the initial concentration on the adsorption efficiency and capacity of the modified apatite ore, the concentration of Co^{2+} solution was varied from 7 to 315 $mg \cdot L^{-1}$, and for the Cr^{3+} solution, the concentration was changed from 5 to 370 $mg \cdot L^{-1}$. Figure 6 shows that when the initial concentration increases, the adsorption efficiency decreases, and the capacity rises. When the initial concentration varies to a definite value, the adsorption capacity has nearly no increment, corresponding to the adsorption process reaching the saturated state. For a given amount of modified apatite ore, there is a specified number of adsorption pores. In the case of all the adsorption pores being filled by Co^{2+} and Cr^{3+} ions, when the concentration of heavy metals increases, the adsorption capacity has nearly no change.
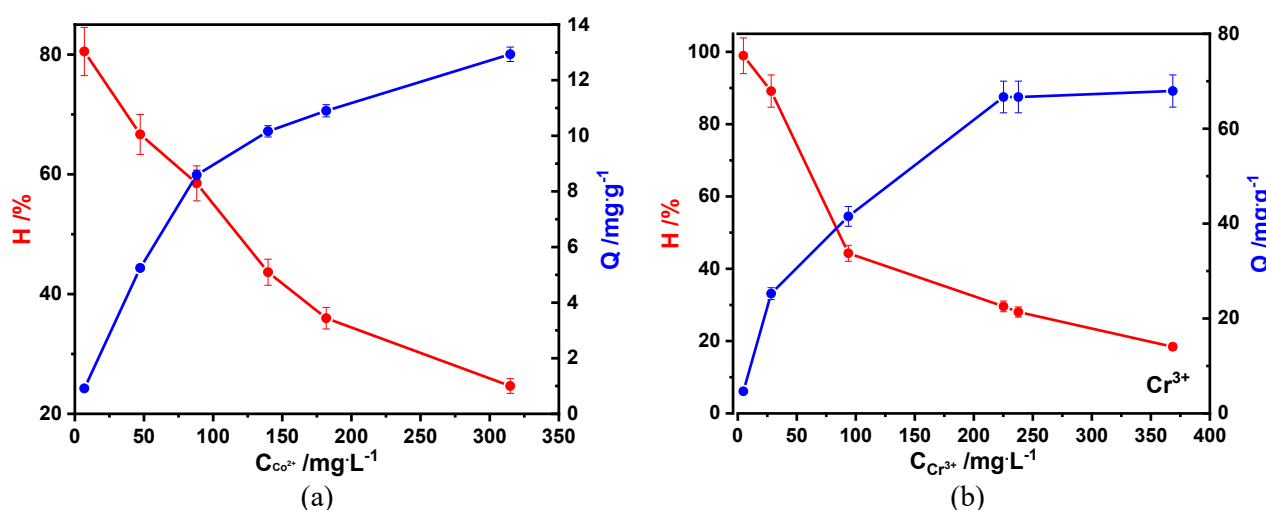

(a)   (b)

Figure 6: The variation of adsorption efficiency and capacity follows the Co^{2+} (a) and Cr^{3+} (b) initial concentration with the mass of modified apatite ore is about 0.3 g and 0.05 g, pH_0, contacting time is about 15 and 60 minutes, respectively.

3.7. Temperature effect studies

When the temperature of the adsorption process increase, the adsorption efficiency and capacity also increase (tables 1 and 2). The intercept and slope of the plot of $\ln(K_d)$ versus $\frac{1}{T}$ (figure 7) give the values of the standard Gibbs free energy change ΔG^0, the enthalpy change ΔH^0 and the entropy change ΔS^0 (tables 3 and 4). A negative value of ΔG^0 and a positive value of ΔH^0 show that the adsorption process is spontaneous and endothermic. The values of ΔG^0 are smaller than the value of physical adsorption (-20 to 0 $kJ \cdot mol^{-1}$) and chemisorption range (-80 to -400 $kJ \cdot mol^{-1}$), suggesting that the adsorption of Co^{2+} and Cr^{3+} onto modified apatite ore is physisorption. The ΔS^0 with positive values proves the increase in randomness at the adsorbate-adsorbant interface.[34]

Table 1: The parameters H (%), Q_e ($mg \cdot g^{-1}$), K_d when temperature varies in Co^{2+} adsorption process (t = 60 minutes, mass of modified apatite ore = 0.1 g, pH_0) (K_d is the equilibrium constant)

Temperature (K)	C_0 ($mg \cdot L^{-1}$)	C_e ($mg \cdot L^{-1}$)	H_{Co} (%)	Q_e ($mg \cdot g^{-1}$)	$K_d = Q_e/C_e$ ($L \cdot g^{-1}$)	$\ln K_d$	1/T (K^{-1})
298		17.83	70.87	21.69	1.22	0.20	0.003356
308	61.20	16.54	72.97	22.33	1.35	0.30	0.003247
338		11.13	81.81	25.03	2.25	0.81	0.002959
348		10.64	82.61	25.28	2.38	0.87	0.002874

Table 2: The parameters H (%), Q_e (mg·g⁻¹), K_d when temperature varies in Cr³⁺ adsorption process
(t = 60 minutes, mass of modified apatite ore = 0.05 g, pH0)

Temperature (K)	C_0 (mg·L⁻¹)	C_e (mg·L⁻¹)	H_{Cr} (%)	Q_e (mg·g⁻¹)	$K_d = Q_e/C_e$ (L·g⁻¹)	$\ln K_d$	1/T (K⁻¹)
308		5.16	82.92	25.04	4.85	1.58	0.003247
317	30.20	1.56	94.83	28.64	18.35	2.91	0.003155
328		0.08	99.75	30.12	399	5.99	0.003049
338		0.05	99.83	30.15	599	6.40	0.002959

Figure 7: The relationship of LnK$_d$ and 1/T in the case of Co²⁺ (a) and Cr³⁺ (b)

Table 3: The parameters ΔH^0, ΔS^0, and ΔG^0 in the case of Co²⁺

Temperature (K)	ΔH^0 (kJ·mol⁻¹)	ΔS^0 (kJ·mol⁻¹·K⁻¹)	$\Delta G^0 = \Delta H^0 - T.\Delta S^0$ (kJ·mol⁻¹)
298			-0.43
308	12.38	0.043	-0.86
338			-2.15
348			-2.58

Table 4: The parameters ΔH^0, ΔS^0, and ΔG^0 in the case of Cr³⁺

Temperature (K)	ΔH^0 (kJ·mol⁻¹)	ΔS^0 (kJ·mol⁻¹·K⁻¹)	$\Delta G^0 = \Delta H^0 - T.\Delta S^0$ (kJ·mol⁻¹)
308			-4.07
318	151.25	0.504	-8.61
338			-14.15
348			-19.20

3.8. Adsorption isotherm

The adsorption experiments were conducted under the following conditions: 0.3 g or 0.05 g of modified apatite ore in 50 mL of Co²⁺ and Cr³⁺ solution with varying concentrations, stirring for 60 minutes with a speed of 400 rpm. The C_e and Q_e parameters were calculated from the experimental data, and Langmuir and Freundlich isotherm adsorption models were established. As can be seen from Figure 8, the Langmuir model can be used to describe the experimental data of Co²⁺ and Cr³⁺ adsorption process by modified apatite ore in research conditions with R^2 values being respectively 0.99399 and 0.97251. This is higher than for the Freundlich model (0.98726 and 0.9704). From the isotherm curve, which follows the Langmuir model, we can calculate that the Co²⁺ maximum adsorption capacity Q_{max} is 13.52 mg·g⁻¹ and the Cr³⁺ maximum adsorption capacity is 70.37 mg·g⁻¹. Table 5 shows the results previously published for comparison with this study about the optimized condition, adsorption capacity, and removal yield. It can be observed that modified apatite ore at the selected optimized

conditions has a better efficiency compared to some   other adsorbents.

Table 5: Comparison of the optimized conditions, removal%, and adsorption capacity of different Co^{2+} and Cr^{3+} adsorbents relative to our modified apatite ore

Adsorbent	Conditions	Adsorption capacity (mg/g)	Removal %	Reference
Wood ash	pH 2 3 hours 100 g/L wood ash	-	Co^{2+} 99 %	[4]
FAU-type zeolite	20 mL 90 minutes 200 mg/L Co^{2+}	Co^{2+} 12.2 mg/g	Co^{2+} 20-65 %	[14]
Hydroxyapatite/chitosan composite	pH 6.0 3 g/L of material 40 minutes 10 mg/L Co^{2+} 25 °C	Co^{2+} 10.63 mg/g	Co^{2+} 88.72 %	[2]
Hydroxyapatite/Fe_3O_4/ polydopamine	pH 6 1 g/L material 25 °C 50 minutes	Co^{2+} 49.32 mg/g	Co^{2+} 90 %	[20]
Modified apatite ore	0.3 g material 50 mL 25 °C 15 minutes	Co^{2+} 13.52 mg/g	Co^{2+} 85 %	This study
Bone char	pH 5 25 °C 30 mg/L Cr^{3+} V = 40 mL 0.2 g BC 7 days	Cr^{3+} 78.59 mg/g	-	[3]
Activated carbon, silica, silica activated carbon composite	20 mL pH 2.0 24 hours 30 ppm	Cr^{3+} 60.9 mg/g	Cr^{3+} 50.6 %	[15]
Hydroxyapatite nanoparticles	1.0 g HAp 250 mL Cr^{3+}	Cr^{3+} 96.9 mg/g	-	[35]
Hydroxyapatite/ carboxymethyl cellulose composite	100 mg/L Cr^{3+}	Cr^{3+} 12.89 mg/g	-	[36]
n-HAp		Cr^{3+} 9.03 mg/g		
Modified apatite ore	0.05 g material 50 mL 25 °C 60 minutes	Cr^{3+} 70.37 mg/g	Cr^{3+} 90 %	This study

3.9. Adsorption kinetics

Figure 9a,b shows the kinetic data using Lagergren's pseudo-first-order equation, and Fig. 9c,d shows the kinetic data plotted by McKay and Ho's pseudo-second-order equation. A linear relationship with a high correlation coefficient (R^2 = 0.99933 and 0.99231) between t/Q_t and t was obtained, which shows the Co^{2+} and Cr^{3+} adsorption on modified apatite ore fitted with the pseudo-second-order model than the pseudo-first-order one. The calculated parameters of this model are presented in table 6.

In addition, there was an agreement between the values of the measured $Q_{e.exp}$ and the calculated ones ($Q_{e.cal}$), resulting from the plots of pseudo-second-

order (table 6) at elaborated Co^{2+} and Cr^{3+} concentration. This also confirmed that the adsorption of Co^{2+} and Cr^{3+} onto modified apatite ore is completely consistent with the pseudo-second-order model.
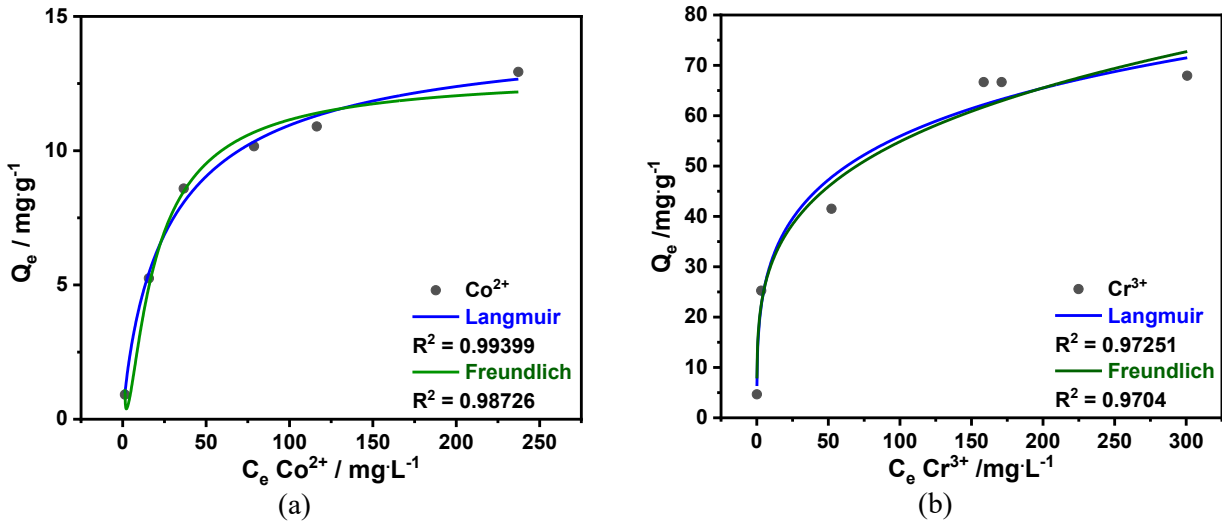

Figure 8: Adsorption isotherm curves of Co^{2+} (a) and Cr^{3+} (b) follow the Langmuir and Freundlich model
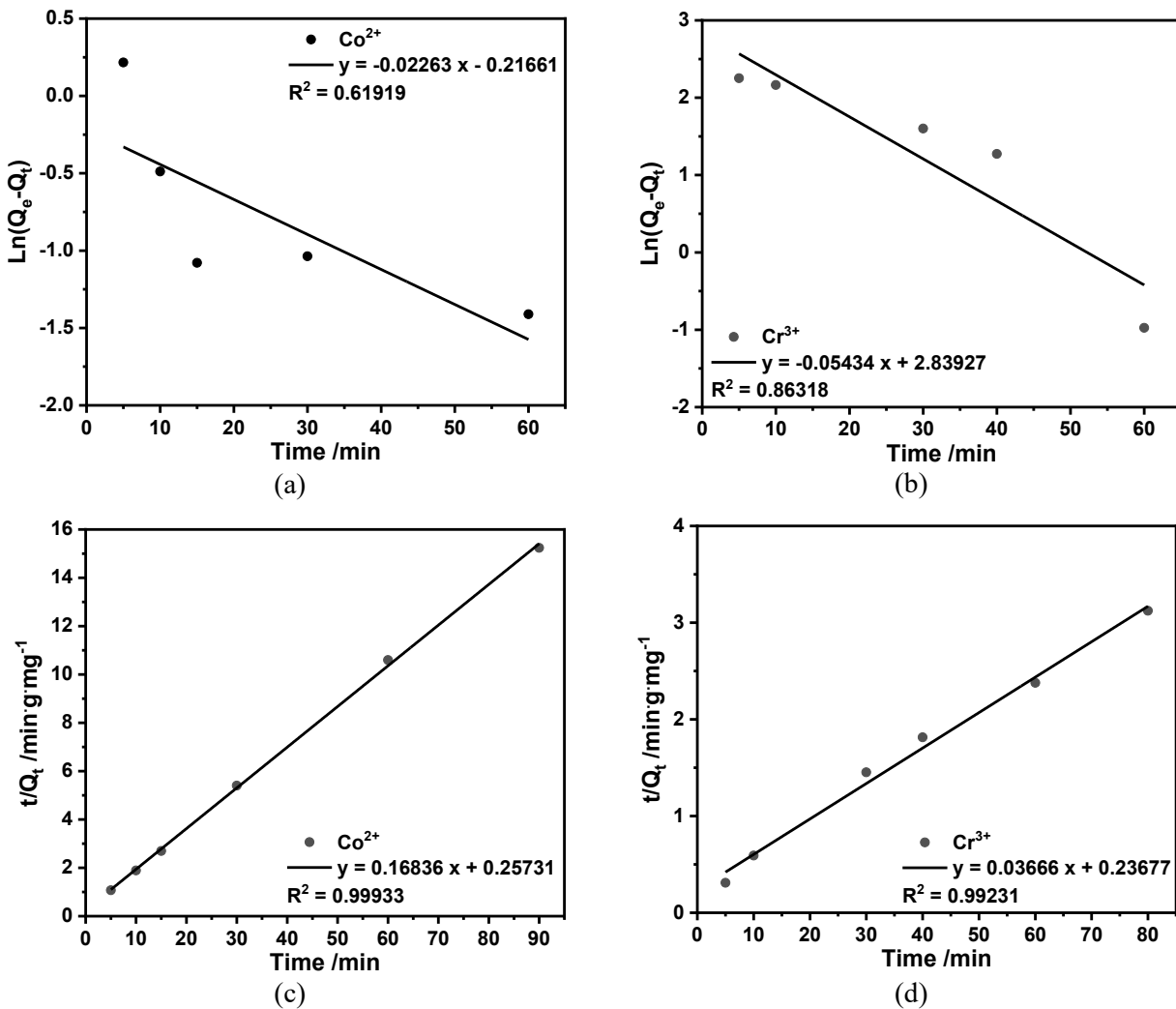

Figure 9: (a, b) Lagergren's pseudo-first-order law, (c, d) McKay and Ho's pseudo-second-order law kinetic models were used to model adsorption data

Table 6: Parameters of Co^{2+} and Cr^{3+} removal process calculated using McKay's and Ho's pseudo-second-order law model (k_2 is the pseudo-second-order rate constant for adsorption)

	Linear equation	Qe.exp $(mg \cdot g^{-1})$	Qe.cal $(mg \cdot g^{-1})$	k_2 $(g \cdot mg^{-1} \cdot min^{-1})$	R^2
Co^{2+}	y = 0.16836 x + 0.25731	5.91	5.94	0.110159	0.99933
Cr^{3+}	y = 0.03666 x + 0.23677	25.62	27.28	0.005676	0.99231

3.10. Wastewater treatment

After the detailed investigation of the heavy metal ions removal based on the model solutions within the application of the nanostructural hydroxyapatite used from the apatite ore, the following step was the application of the proposed material for the removal of heavy metal ions from the real wastewater collected at a plating company in Noi Bai Industrial Zone, Trieu Khuc craft village, Hanoi, and at a lake of wastewater number 2 – Lung Vang mine (Pb-Zn), Bac Kan, Vietnam. Based on the results presented in Tab. 7 it is seen that the plating sample contains Co^{2+} and Cr^{3+}, besides there are some other heavy metal ions such as Cu^{2+} and Zn^{2+}, where the concentration of Cr^{3+}, Cu^{2+}, and Zn^{2+} in plating wastewater is much higher than the maximum permitted limit concentration of industrial wastewater following the QCVN 40:2011/BTNMT norm (1 $mg \cdot L^{-1}$; 1 $mg \cdot L^{-1}$ and 2 $mg \cdot L^{-1}$, corresponding). In the case of craft village and mine wastewater, there is the presence of Cr^{3+} and Zn^{2+} ions but the concentration is very small.

Through the optimized parameters of the sorbent, the experiments were performed in the following conditions: 0.03 g; 0.1 g; 0.2 g; 0.3 g and 1 g of modified apatite ore were placed in 50 mL of wastewater primarily filtered to remove solid impurities suspended in the solution. After the filtration, the adsorbent was stirred for 60 minutes likewise the experiments described above. Then, the sample was centrifuged to separate the adsorbent from the suspension and the solution was tested with the application of the AAS technique. Besides, the pH of the plating wastewater is very low, out of the range for industrial wastewater (pH 5.5-9.0). After treatment with 0.03 g modified apatite ore, the craft village and mine wastewater have heavy metal ion concentration and pH values in the range of above norm. However, with plating wastewater, the heavy metal ion concentration decreases the pH increase but is still much higher compared to the limited value. Therefore, the higher dose of modified apatite ore was used, namely, 0.1 g; 0.2 g; 0.3 g; and 1 g. When the dose of adsorbent increases, the concentration of heavy metal ions decrease, and pH increase. With the dose of modified apatite ore of 1 g, the concentration of heavy metal ions and pH is in the range of norm. Based on the obtained results on Table 8, it is seen that the modified apatite ore can be used as an effective absorbent for heavy metals removal from the wastewater. Its application also can be used on a larger, industrial scale.

Table 7: The values of concentration and pH of real wastewater samples

Wastewater	Co^{2+} $(mg \cdot L^{-1})$	Cr^{3+} $(mg \cdot L^{-1})$	Cu^{2+} $(mg \cdot L^{-1})$	Zn^{2+} $(mg \cdot L^{-1})$	pH
Plating	0.036	**12.46**	**7.012**	**16.514**	**2.70**
Craft village	-	0.045	-	-	7.54
Mine	-	0.023	-	0.083	7.63

Table 8: The values of concentration, H and pH of real wastewater samples after treatment

Mass	Wastewater	Co^{2+} $(mg \cdot L^{-1})$	$H_{Co^{2+}}$ (%)	Cr^{3+} $(mg \cdot L^{-1})$	$H_{Cr^{3+}}$ (%)	Cu^{2+} $(mg \cdot L^{-1})$	$H_{Cu^{2+}}$ (%)	Zn^{2+} $(mg \cdot L^{-1})$	$H_{Zn^{2+}}$ (%)	pH
0.03 g	Plating	0.018	50	**10.648**	14.55	**5.277**	24.74	**13.923**	15.69	**3.74**
	Craft village	-	-	0.023	50	-	-	-	-	7.9
	Mine	-	-	0.023	-	-	-	0.013	84.21	7.4
0.1 g	Plating	-	-	**8.496**	31.82	**2.639**	62.37	**9.421**	42.95	**4.53**
0.2 g	Plating	-	-	**4.169**	66.55	0.318	95.46	**3.101**	81.22	**4.80**
0.3 g	Plating	-	-	**2.719**	78.18	0.175	97.51	**2.117**	87.18	**4.87**
1 g	Plating	-	-	0.400	97.27	-	-	0.088	99.47	5.60

3.11. Crystallinity analysis

Complementary to AAS measurements, the modified apatite ore was investigated with X-ray diffraction (XRD) to estimate the crystallinity and chemical composition of the sorbent used for the heavy metals removal. Figure 10 presents the XRD patterns of modified apatite ore before and after the adsorption of Co^{2+} (at pH_0, m = 0.3 g, 15 minutes, Co^{2+} concentration of 30 mg·L^{-1}) and Cr^{3+} (pH_0, m =

0.05 g, 60 minutes, Cr^{3+} concentration of 30 ppm). Modified apatite ore has characteristic peaks of hydroxyapatite with the highest intensity peak at around 32.5° and another peak at about 26.2°. After the adsorption process with Co^{2+} and Cr^{3+}, the obtained material presents only characteristic peaks of hydroxyapatite; this result indicates that the phase structure of the material does not change leading to the desorption and reused ability of the material.
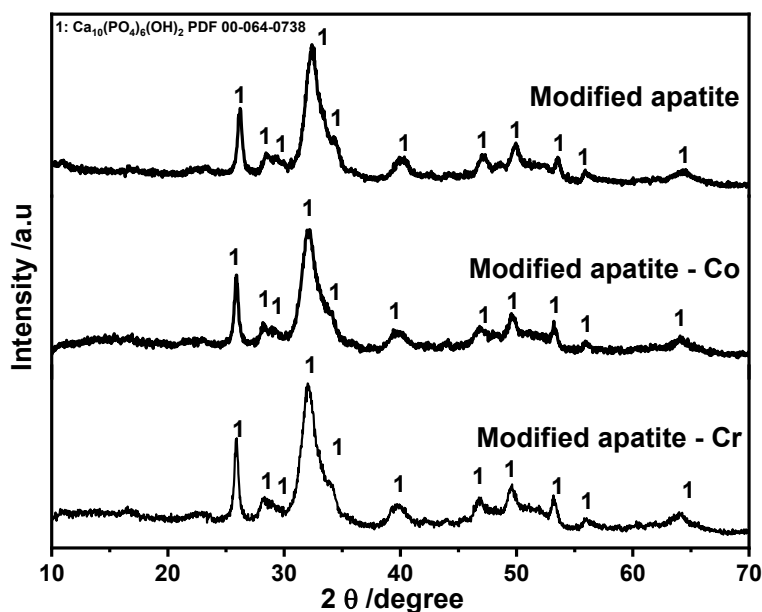

Figure 10: XRD patterns of modified apatite ore before and after the adsorption of Co^{2+} and Cr^{3+}

4. CONCLUSIONS

Modified apatite ore shows a huge potential in water remediation from heavy metal pollution. Within the application of the natural apatite ore sources, it became a low-cost material that effectively deals with water pollution. In this work, we have presented its effective application in the removal of heavy metal ions from the wastewater gained from the mine. Prior to the wastewater treatment, it has been measured that the suitable conditions for this application are 0.3 g of modified apatite ore adsorbing 50 mL of Co^{2+} solution of 30 mg·L^{-1} at pH_0 and a contacting time of 15 minutes. With Cr^{3+}, the amount of modified apatite ore is 0.05 g to adsorb 50 mL of Cr^{3+} solution of 30 mg·L^{-1} at pH_0, and the preferable contacting time is 60 minutes; the adsorption process matches the Langmuir isotherm model with a maximum capacity is 13.52 mg·g^{-1} for Co^{2+} and 70.37 mg·g^{-1} for Cr^{3+}. The kinetic data of the adsorption process fitted better with the pseudo-second-order model than the pseudo-first-order one. The adsorption process is physisorption with

enthalpy change of 12.38 and 151.25 kJ·mol^{-1} for Co^{2+} and Cr^{3+}, respectively.

Conflict of interest. *The authors declare no competing interests.*

REFERENCES

1. V. Dauvalter. Heavy metal concentrations in lake sediments as an index of freshwater ecosystem pollution, Disturbance and Recovery in Arctic Lands: An Ecological Perspective, Ed. by Crawford RMM, Dordrecht: Kluwer Academic Publishers, **1997**, 333-351.
2. N. Gupta, A. K. Kushwaha, M. C. Chattopadhyaya. Adsorptive removal of Pb^{2+}, Co^{2+} and Ni^{2+} by hydroxyapatite/chitosan composite from aqueous solution, *J. Taiwan Inst. Chem. Eng.*, **2012**, *43*, 125-131.
3. J. V. Flores-Cano, R. Leyva-Ramos, F. Carrasco-

Marin, A. Aragón-Pina, J. J. Salazar-Rabago, S. L. Ramos. Adsorption mechanism of Chromium(III) from water solution on bone char: effect of operating conditions, *Adsorption*, **2016**, *22*, 297-308.

4. M. Malakootian, A. Almasi, H. Hossaini. Pb and Co removal from paint industries effluent using wood ash, *Int. J. Environ. Sci. Tech.*, **2008**, *5(2)*, 217-222.

5. L. Laura, V. Bart, V. D. S. Catherine, W. Floris, M. Leen. Cobalt toxicity in humans - A review of the potential sources and systemic health effects, *Toxicology*, **2017**, *387*, 43-56.

6. R. Shrestha, S. Ban, S. Devkota, S. Sharma, R. Joshi, A. P. Tiwari, H. Y. Kim, M. K. Joshi. Technological trends in heavy metals removal from industrial wastewater: A review, *J. Environ. Chem. Eng.*, **2021**, *9(4)*, 105688.

7. M. Elie, A. Rahdar, G. Z. Kyzas. Sawdust for the removal of heavy metals from water: a review, *Molecules*, **2021**, *26(14)*, 4318.

8. L. Joseph, B. M. Jun, J. R. V. Flora, C. M. Park, Y. Yoon. Removal of heavy metals from water sources in the developing world using low-cost materials: A review, *Chemosphere*, **2019**, *229*, 142-159.

9. S. Honarparvar, X. Zhang, T. Chen, A. Alborzi, K. Afroz, D. Reible. Frontiers of membrane desalination processes for brackish water treatment: A review, *Membranes*, **2021**, *11(4)*, 246.

10. L. T. Duyen, L. T. P. Thao, D. T. Hai, P. T. Dung, P. T. Nam, N. T. Thom, C. T. Hong, C. T. Linh, D. T. M. Thanh. Removal of Cd^{2+} by hydroxyapatite adsorption granule from aqueous solution, *Vietnam J. Chem.*, **2018**, *56(5)*, 542-547.

11. P. T. Nguyen, X. T. Nguyen, T. V. Nguyen, T. T. Nguyen, T. Q. Vu, H. T. Nguyen, N. T. Pham, T. M. T. Dinh. Treatment of Cd^{2+} and Cu^{2+} ions using modified apatite ore, *J. Chem.*, **2020**, *2020*, 6527197.

12. A. Vahdat, B. Ghsemi, M. Yousefpour. Synthesis of hydroxyapatite and hydroxyapatite/Fe_3O_4 nanocomposite for removal of heavy metals, *Environ. Nanotechnol. Monit. Manag.*, **2019**, *12*, 100233.

13. M. E. Ali, M. E. Hoque, S. K. S. Hossain, M. C. Biswas. Nanoadsorbents for wastewater treatment: next generation biotechnological solution, *Int. J. Environ. Sci. Tech.*, **2020**, *17*, 4095-4132.

14. I. V. Joseph, L. Tosheva, A. M. Doyle. Simultaneous removal of Cd(II), Co(II), Cu(II), Pb(II), and Zn(II) ions from aqueous solutions via adsorption on FAU-type zeolites prepared from coal fly ash, *J. Environ. Chem. Eng.*, **2020**, *8(4)*, 103895.

15. M. Karnib, A. Kabbani, H. Holail, Z. Olama. Heavy metals removal using activated carbon, silica and silica activated carbon composite, *Energy Procedia*, **2014**, *50*, 113-120.

16. V. B. Yadav, R. Gadi, S. Kalra. Clay based nanocomposites for removal of heavy metals from water: A review, *Journal of Environmental Management*, **2019**, *232*, 803-817.

17. S. Li, S. Li, N. Wen, D. Wei, Y. Zhang. Highly effective removal of lead and cadmium ions from wastewater by bifunctional magnetic mesoporous silica, *Sep. Purif. Technol.*, **2021**, *265*, 118341.

18. P. T. Nam, D. T. M. Thanh, N. T. Phuong, N. T. T. Trang, C. T. Hong, V. T. K. Anh, T. D. Lan, N. T. Thom. Adsorption of Ag^+ ions using hydroxyapatite powder and recovery silver by electrodeposition, *Vietnam J. Chem.*, **2021**, *59(2)*, 179-186.

19. A. Pooladi, R. Bazargan-Lari. Simultaneous removal of copper and zinc ions by Chitosan/ Hydroxyapatite/ nano-Magnetite composite, *J. Mater. Res. Technol.*, **2020**, *9(6)*, 14841-14852.

20. R. Foroutan, S. J. Peighambardoust, A. Ahmadi, A. Akbari, S. Farjadfard, B. Ramavandi. Adsorption mercury, cobalt, and nickel with a reclaimable and magnetic composite of hydroxyapatite/Fe_3O_4/ polydopamine, *J. Environ. Chem. Eng.*, **2021**, *9(4)*, 105709.

21. Y. Zhou, W. Li, X. Jiang, Y. Sun, H. Yang, Q. Liu, Y. Cao, Y. Zhang, H. Cheng. Synthesis of strontium (Sr) doped hydroxyapatite (HAp) nanorods for enhanced adsorption of Cr(VI) ions from wastewater, *Ceram. Int.*, **2021**, *47(12)*, 16730-16737.

22. G. N. Kousalya, M. R. Gandhi, C. S. Sundaram, S. Meenakshi. Synthesis of nano-hydroxyapatite chitin/chitosan hybrid biocomposites for the removal of Fe(III), *Carbohydr. Polym.*, **2010**, *82*, 594-599.

23. K. Bouiahya, I. Es-saidi, C. E. Bekkali, A. Laghzizil, D. Robert, J. M. Nunzi, A. Saoiabi. Synthesis and properties of alumina-hydroxyapatite composites from natural phosphate for phenol removal from water, *Colloids Interface Sci. Commun.*, **2019**, *31*, 100188.

24. E. Shorki, B. Khanghahi, E. Esmizadeh, H. Etemadi. Biopolymer-based adsorptive membrane for simultaneous removal of cationic and anionic heavy metals from water, *Int. J. Environ. Sci. Technol.*, **2022**, *19*, 4167-4180.

25. N. S. De Resende, C. L. M. Camargo, P. C. Reis, C. A. C. Perez, V. M. M. Salim. Mechanisms of mercury removal from aqueous solution by high-fixation hydroxyapatite sorbents, *Int. J. Environ. Sci. Technol.*, **2019**, *16*, 7221-7228.

26. P. V. Thi, N. P. Thi, P. T. Nguyen, H. D. Thi, T. D. T. Mai. Deflouridation behavior of nano Zn-Hydroxyapatite synthesized by chemical precipitation method, *Vietnam J. Chem.*, **2012**, *50(6B)*, 99-105.

27. G. Tomar, A. Thareja, S. Sarkar. Enhanced fluoride removal by hydroxyapatite-modified activated alumina, *Int. J. Environ. Sci. Tech.*, **2015**, *12*, 2809-2818.

28. W. Wei, R. Sun, Z. Jin, J. Cui, Z. Wei. Hydroxyapatite-gelatin nanocomposite as a novel absorbent for nitrobenzene removal from aqueous solution, *Appl. Surf. Sci.*, **2014**, *292*, 1020-1029.

29. M. Harja, G. Ciobanu. Studies on adsorption of oxytetracycline from aqueous solution onto hydroxyapatite, *Sci. Total Environ.*, **2018**, *628-629*, 36-43.

30. Y. Chen, T. Lan, L. Duan, F. Wang, B. Zhao, S. Zhang, W. Wei. Adsorptive removal and adsorption kinetics of fluoroquinolone by nano-

hydroxyapatite, *PlOS one*, **2015**, *10(12)*, e0145025.

31. M. Harja, G. Ciobanu. Removal of oxytetracycline from aqueous solutions by hydroxyapatite as a low-cost adsorbent, *E3S Web of Conferences. EDP Sciences*, **2017**, *22*, 00062.

32. C. E. Bekkali, J. Labrag, A. Oulguidoum, I. Chamkhi, A. Laghzizil, J. M. Nunzi, D. Robert, J. Aurag. Porous ZnO/hydroxyapatite nanomaterials with effective photocatalytic and antibacterial activities for the degradation of antibiotíc, *Nanotechnol. Environ. Eng*, **2022**, *7*, 333-341.

33. A. Ragab, I. Ahmed, D. Bader. The removal of brilliant green dye from aqueous solution using nano hydroxyapatite/chitosan composite as a sorbent, *Molecules*, **2019**, *24*, 847.

34. T. T. L. Thi, H. S. Ta, K. L. Van. Activated carbons from coffee husk: preparation, characterization, and reactive red 195 adsorption, *J. Chem. Res.*, **2021**, *2021,* 380-394.

35. Y. Si, J. Hou, H. Yin, A. Wang. Adsorption kinetics, isotherms, and thermodynamics of Cr(III), Pb(II), and Cu(II) on porous hydroxyapatite nanoparticles, *J. Nanosci. Nanotechnol.*, **2018**, *18*, 3484-3491.

36. Z. Abbasi, E. Ramezani, A. Farrokhnia, A. S. Shahraki, A. A. Naseri. Hydroxyapatite/ carboxymethyl cellulose composite: synthesis, characterization, kinetic, thermodynamic study for removal of Cr(III), *Alkhas*, **2021**, *3(1)*, 12-17.

Corresponding authors: **Nguyen Thu Phuong**
Department of Corrosion and Protection of Metals
Institute for Tropical Technology
Vietnam Academy of Science and Technology
18 Hoang Quoc Viet, Cau Giay, Hanoi 10000, Viet Nam
E-mail: ntphuong@itt.vast.vn
Tel: +84- 982924405.

Dinh Thi Mai Thanh
University of Science and Technology of Hanoi
Vietnam Academy of Science and Technology
18 Hoang Quoc Viet, Cau Giay, Hanoi 10000, Viet Nam
E-mail: dtmthanh@itt.vast.vn
Tel: +84- 914256885.